
Plastic Composites Using Mango Leaf Waste for Cost Effectiveness and Green Environment

Rahmat Satoto^{1*}, Rijal Ahmadi², Dadi Rusdiana³, Erni Ernawaty³, Anung Syampurwadi¹, Akbar Hanif Dawam Abdullah¹

¹ Research Unit for Clean Technology, National Research and Innovation Agency Republic Indonesia. Kompleks LIPI, Jalan Sangkuriang, Bandung 40135, Indonesia

² Materials Science and Engineering Department, Institut Teknologi Bandung, Bandung 40132, Indonesia

³ Department of Physics Education, Universitas Pendidikan Indonesia, Jl. Dr. Setiabudi No. 229, Bandung 40154, Indonesia

*Corresponding author: rsatoto@yahoo.com

Received: January 2022; Revision: February 2022; Accepted: March 2022; Available online: May 2022

Abstract

Due to ecological considerations, natural biodegradation composites are widespread in tailoring plastics properties to specific needs. This work aims to demonstrate the available opportunity in using 100 and 140 mesh powdered mango leaf (PML) waste as a filler in polypropylene (PP) composites. Composites were produced via melt blending on a twin-screw internal mixer, with a different particulate size and a weight ratio of PML. Morphology, tensile, flexural, hardness, tear, puncture, thermal, and water absorption properties of the composites were assessed after 0, 1, 7, 14, and 28 days of water immersion. We found that the smaller particle size shows a better mechanical and water absorption of the composites, but not for thermal properties. The mechanical properties decreased with increasing PML content; however, these properties did not differ considerably from pure PP and other composites with natural filler. Besides, these polypropylene/PML composites showed excellent properties in water absorption.

Keywords: Mango leaf, Mechanical properties, Natural fiber, Polypropylene composite, Single-used articles.

DOI: 10.15408/jkv.v8i1.24557

1. INTRODUCTION

Increasing concern on environmental issues and law enforcement have stimulated a growing interest in demand for eco-friendly materials (Amin et al., 2019; Marichelvam et al., 2019). As a result, many research activities were directed at bio-based polymers such as thermoplastic starch (TPS) as alternative renewable sources to replace fossil-based polymers. Thermoplastic starch seems to be very promising and cost-competitive among bio-based materials considering its availability in various vegetations (Amin et al., 2019; Marichelvam et al., 2019; Mazerolles et al., 2019). However, starch-based materials have some disadvantages, such as stability, aging, low water resistance, and poor mechanical properties (Delville et al., 2003; Nguyen et al., 2016), so their application needs to be investigated. Research to develop and expand

the usability of starch based-polymer materials is in progress. Nowadays, starch based-polymer materials' usability is still being developed in many studies (Nguyen et al., 2016; Medina-Jaramillo et al., 2017).

The biomass could be beneficial in lower energy consumption and overall emission from environmental contamination. Therefore, the biomass could be blended with polymer composites as fillers, reducing the volume of plastics in a composite as an alternative approach to utilizing bio-based material (Satoto et al., 2019). A polymer composite consists of a polymer matrix and fillers to serve specific objectives of the engineering materials. Better thermal stability has been reported on lignin/polyethylene blends, where lignin is a non-food natural filler (Wang et al., 2016; Sadeghifar &

Argyropoulos, 2016). Blending rice husk with polyethylene showed a decrease in bending and tensile strength (Zhang et al., 2018), but the modulus was increased (Bilal et al., 2014). Another study has been done to manipulate the hydrophobicity of the mixtures with cellulose/polyethylene blends (Dordević et al., 2016).

Polymeric biocomposites of pineapple (Kengkhetkit & Amornsakchai, 2014; Indra Reddy et al., 2018) and palm leaf fibers have also been prepared (Kocak & Mistik, 2015). Leaves can be one option to obtain non-wood natural fibers other than various parts of plants such as fruit, stem, and seed (Abdullah & Aslan, 2019). However, the use of non-fiber leaves for polymer composites is still limited. Non-fiber leaves can benefit from processing/treatment since no fiber extraction is needed and are available at a low cost (Scaffaro et al., 2018). So far, utilizing mango leaves for degradation filler in composites is not published yet. Mango leaf contains 27.16% cellulose, 53.98% hemicellulose, and 18.85% lignin, similar to natural fiber (Das et al., 2013). Moreover, many mango tree varieties are found all over the country of Indonesia. Therefore, using mango leaves (as a by-product) will help to reduce waste and environmental contaminants.

Since its application is versatile, polypropylene (PP) is widely utilized for single-used articles such as packaging, wrapping, and bathroom amenity. Consequently, the waste of PP single used articles will be comparable to its production. The waste may only be landfilled or incinerated. The landfilled PP contaminates the environment for a relatively long time since its low degradation rate in nature. Mango leaf powder blended with PP was thought of as a degradation agent in the composites so that the waste extinguishing in landfills would be fastened.

This research aims to prepare and characterize polypropylene/powdered mango leaves (PP/PML) composites. The study was done to understand the effect of different powdered mango leaves particle size and composition on mechanical properties, physical properties, thermal properties, and morphology of PP/PML composites. In addition, it is essential to identify the actual potential of PP/PML composites for possible future applications for single-used articles such

as lunch boxes, wraps, cups, or bathroom amenities.

2. MATERIALS AND METHODS

Materials

Fallen mango leaves were collected from Bandung area, West Java, Indonesia, in 2017. Then the mango leaves were washed using water and dried in a room without heating. The leaves were then crushed and sieved with 140 and 100 mesh. Before melting blended, powdered mango leaves (PML) were air heat-dried for at least 24 hrs at 105 °C until the constant weight to keep low water content. Polypropylene (PP) lot number HI₁₀HO was purchased from PT. Chandra Asri Petrochemical, Tbk. PP melting temperature measured at a heating rate of 5 °C/min by Differential Scanning Calorimetry (DSC) was 163 °C. The maker claimed that the PP contained an undisclosed composition of conventional thermal stabilizers.

PP/PML Preparation

An Internal Mixer (Labo Plastomill Model 30R150, Toyo Seiki Ltd. Japan) was utilized for preparing PP/PML composites by melt blended method. The 12 (twelve) PP/PML composites with different PML particle size (140 and 100 mesh) and content (0, 10, 15, 20, 25, and 30 w/w) were prepared at the setup temperature of 180 °C. The rotation of double-blades was adjusted at 50 rpm, for a time mixture of 8 min. The resulting compounds were then hot-pressed at 190 °C, a pressure of 50 kg/cm², for 8 min, using a hot-press (Gonno, ø152 mm, cap. 37 ton). The hot-pressed compounds are soon quenched using a double-plates press. The PP/PML composites of ca. 120×120×0.23 mm were cut into specimens for tensile, puncture, and tear strength tests. Samples for flexural and hardness tests were prepared 5 mm thick.

Characterization

The samples were prepared under cryo-fractured to observe PML dispersion and interfacial bonding between the polymer matrix PP and filler PML on the composites. A gold coating was applied to prevent electrostatic charging from obtaining a good micrograph. The observation was taken on the outer part or surface and the cut part or edge of the samples. The morphologies were taken using a Scanning Electron Microscope (SEM,

JSM IT-300, Japan) at an acceleration voltage of 10 kV.

Tensile, flexural, puncture and tear tests were performed using the Universal Testing Machine, Model UCT-5T. Tensile and flexural tests were performed according to ISO 527-2 and ASTM D790 standards. The tensile speed was set to 5 mm/min. Measurement of flexural strength was performed following procedure B since the samples did not break after the flexural strain of more than 5%. Puncture and tear resistance tests were carried out according to ASTM D4833 and ASTM D1004. The hardness of samples was measured using a ball indenter of 12.7 mm, minor load, and significant loads of 10 and 60 kg, respectively. The hardness reading was taken 15 s after releasing major to minor loads following ASTM D785. Rockwell Hardness scale R (HRR) measurement was performed using machine Matsuzawa Mrk-M. Each PP/PML composite formulation for every property was tested in five specimens.

The effect of PML content on physical properties was evaluated on water absorption of the composites according to ASTM D570. The composites sheets were cut into specimens of size 76.2×25.4 mm. Five specimens of each

composition were oven-dried at 50 °C for 24 hrs and then immersed in distilled water for a specific time and maintained at room temperature. The samples were taken out at regular time intervals and wiped to measure the water absorption. The amount of water absorbed was determined by measuring the mass difference between the initial and after immersed in water. Thermogravimetric analysis of all PP/PML composites was evaluated using TGA Netzsch TG 209 F1 Libra. The samples with an average mass of 9 mg were heated at 40–550 °C with a heating rate of 10 °C/min under an inert atmosphere (flow rate 20 mL/min gas N₂). The effect of PML on the thermal stability of the composites was observed as that of pure PP.

3. RESULTS AND DISCUSSION

The PP/PML composites containing different particle sizes and amounts of PML have been prepared, and their mechanical properties were observed and evaluated.

Figure 1 and

Figure 2 display the morphology of the cross-section and surface part of the samples.

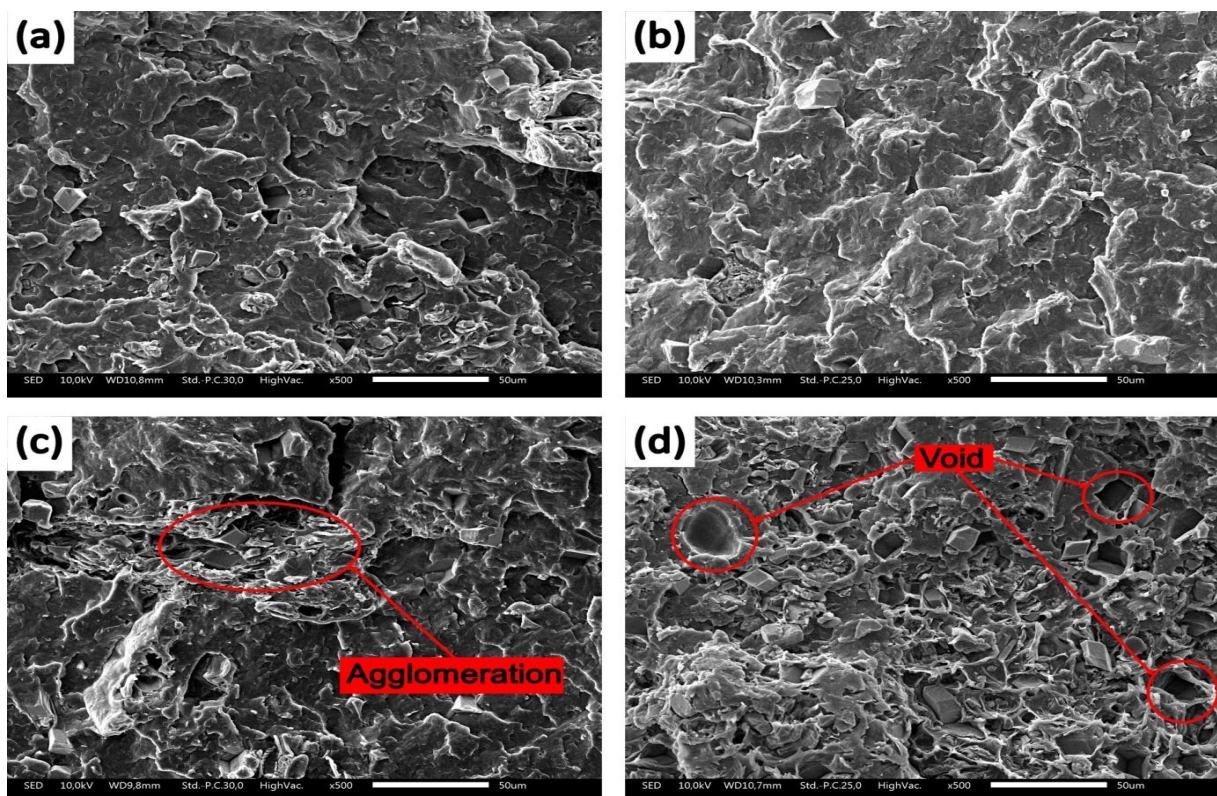


Figure 1. SEM image of cross-section composites: (a) 15 wt% PML 100 mesh, (b) 15 wt% PML 140 mesh, (c) 30 wt% PML 100 mesh, and (d) 30 wt% PML 140 mesh.

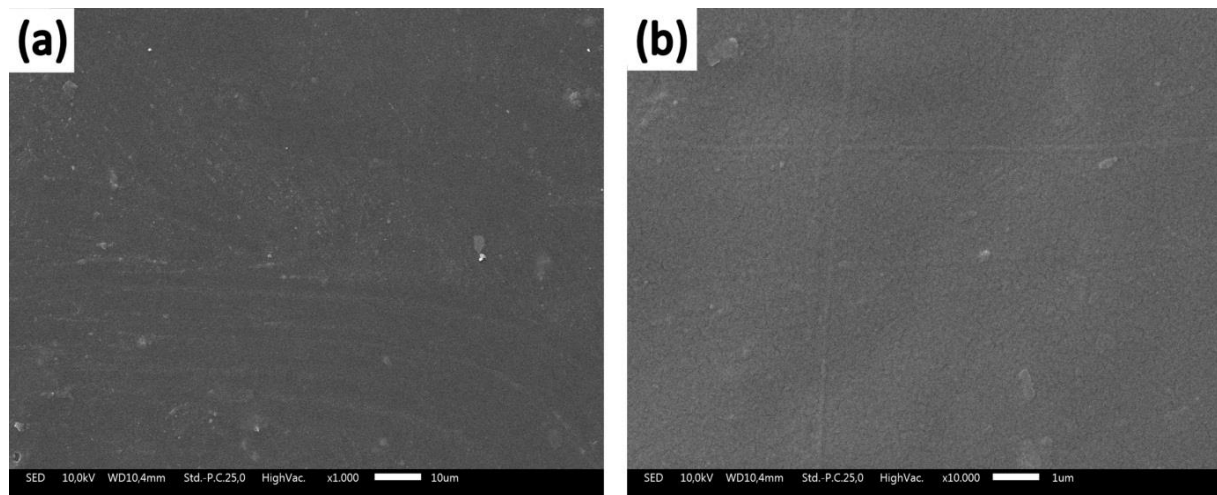


Figure 2. SEM image surface: (a) 15 wt% PML 100 mesh (b) 30 wt% PML 140 mesh.

Morphology

The final product properties of plastic composites depend strongly on their morphology. The major component forms a continuous matrix in most composites, whereas the minor component is the dispersed phase. The continuity of both components may be obtained depending on the nature of the components and the preparation conditions. It was observed that PML always formed a dispersed phase in the composites. Figure 1 shows the cross-section (cryo-fractured) of PP/PML composites at different PML content for both 100 and 140 mesh. The matrix and filler are distinguishable in the cross-section composite micrograph attributed to weak interfacial bonding between the PML particle and PP matrix. It was observed that the PML is not finely dispersed, and at the boundary, PP-PML was observed in some micro-voids. In this composite system, there are some agglomerations in the SEM images of the 100 mesh PP/PML composites (Figure 1c). The more uniform dispersion of PML can be seen in 140 mesh PP/PML composites with the lower contents of PML (Figure 1b).

Figures 2a and 2b show the composites' surface under different magnification. On these surfaces, the PML is not observed, and PP dominates the skin of composites. Such a morphology is good for hindering PML particles from contacting water.

Mechanical Properties

Figure 3 shows the data on tensile strengths of PP and its blend at different PML

contents and particle sizes. A decreasing trend was observed from pure PP to 30 wt% PML content for 100 and 140 mesh. The weak interfacial adhesion between the PP matrix and the filler is the leading cause of tensile strength loss. When compared to the cohesiveness between PP molecules, PML-PP adhesion is poor. Due to poor stress transfer from the PP matrix to the PML filler, the tensile strength of the composites decreased as the PML content increased, and the PML filler created a discontinuous phase in the composites. However, 140 mesh PML composites' tensile strengths were higher than 100 mesh PML composites due to the more acceptable particle size in 140 mesh PML, resulting in a smaller discontinuous phase in the composites. A larger particle may result in more void in the composites. The voids, in turn, will reduce any mechanical property. These 140 mesh PP/PML composites have greater tensile strength than non-fiber pineapple leaves/PP blend (Kengkhetkit & Amornsakchai, 2014) and untreated coir/PP blend (Mir *et al.*, 2013) prepared by others.

Figure 4 shows that all elastic modulus of PP/PML composites were higher than the elastic modulus of pure PP but were not indicate a significant change with increasing PML contents. It suggests that PML provides stiffness to the composites, which are resulted from the inclusion of rigid filler particles into the PP matrix. The highest elastic modulus of PP/PML composite was observed in 140 mesh PML at 25 wt% PML content, with 52% improvement compared to the elastic modulus of pure PP.

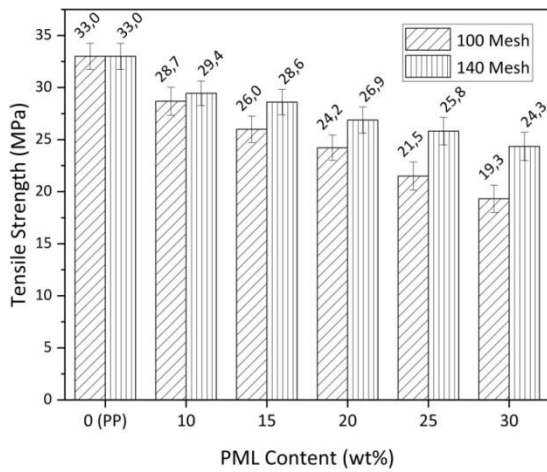


Figure 3. Tensile strength of PP/PML composites

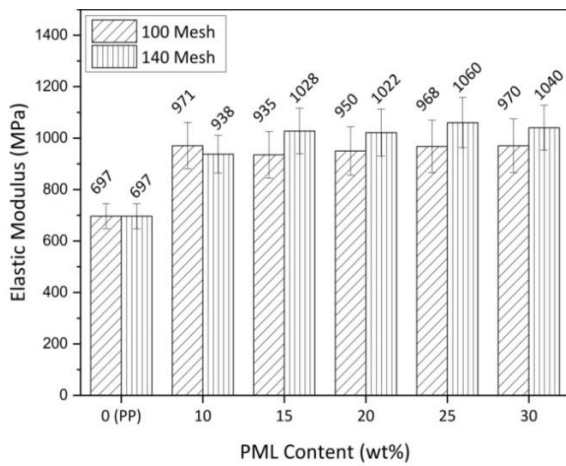


Figure 4. Elastic modulus of PP/PML composites

The higher PML contents result in a less homogeneous and less-effective cross-sectional area of continuous phase PP matrix in the composites. It is a general phenomenon observed in thermoplastics filled with natural filler. The interfacial area and weakening bonding between the filler and the matrix increase as filler content increases. The composites' tensile properties depend strongly on pull-stretch force among the composite components.

The flexural strength of PP/PML composites is shown in Figure 5. The test was performed with procedure B, ASTM D790. However, the samples did not break within the required 5% strain limit. So, the flexural strength is determined as the flexural stress at the strain of 5%. The flexural strength of PP/PML composites for all PML compositions with 140 mesh PML was lower than that of

pure PP and showed a decreasing trend with increasing PML contents. The flexural strength of 100 mesh PP/PML composites was increased for 10 wt% PML content and then decreased from 15 to 30 wt%. However, the flexural strengths for 10, 15, and 20 wt% PML contents were higher than pure PP. A similar trend was also reported by another researcher who studied Jute/PP composites (Ahmed et al., 2014). The flexural data show the composites are good flexibility since they did not break at 5% flexural strain.

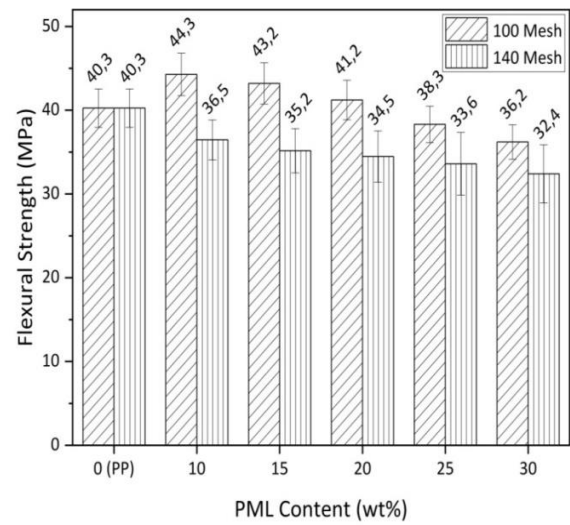


Figure 5. Flexural strength of PP/PML composites

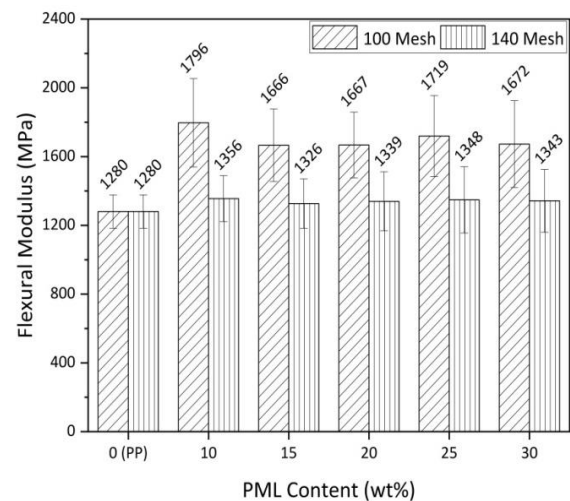


Figure 6. Flexural modulus of PP/PML composites

Figure 6 shows the flexural modulus of a PP/PML composite at various PML content levels. Their flexural modulus is higher than pure PP, particularly at 100 mesh PML, but it

appears to be unaffected by PML concentration. The composite with 10% PML content has the most excellent flexural modulus of 1796.4 MPa. These results are higher than the flexural modulus of potato starch/PP composites (Roy et al., 2011) but lower than jute/PP composites (Rahman et al., 2008). The flexural modulus of 140 mesh PP/PML composites was not significantly improved, even though a slight increment was observed. The nature of flexural and tensile testing is a bit different. A half-upper specimen suffers compression force in flexural testing, while a half-bottom specimen in thickness suffers pulling force. In such testing phenomena, the hardness filler component improves flexural properties. The compression and pull-stretch forces governed the flexural properties of the composites among the composites constituent.

The hardness of a composite material refers to its resistance to shape change when force is applied to it. For composites, it depends on the distribution of the particles into the matrix. Figure 7 shows that the average hardness of the PP/PML composites slightly decreased with PML contents. The hardness reduction on 140 mesh PML was more significant than on 100 mesh PML. These facts could be attributed to the poor interfacial adhesion of the PP matrix and the PML filler. The lower PML contents may produce a composites mixture that is more homogeneous. The physical condition of PML is powders which no bonding among the powders grain, so they do not have HRR. The HRR reduces as the content of PML increases because of very poor back pressure-stress from the filler during loading indenter on the HRR measurement.

Tear strength is the ultimate force required to tear the composite sheets divided by the sample thickness. It is shown in Figure 8 that the tear strength of PP/PML composites linearly decreased with the increase in the PML contents. The tear strength of PP/PML composites, in general, decreased with the increase of PML contents, and they are slightly smaller than the tear strength of PP. For 100 and 140 mesh of 30 wt% PML contents, the tear strength is 165 N/mm and 175 N/mm, respectively. These data conclude that particle size has no significant effect on the tear strength of the PP/PML composites. A similar trend to tensile strength is observed, indicating

that slight filler-matrix adhesion decreases tear strength.

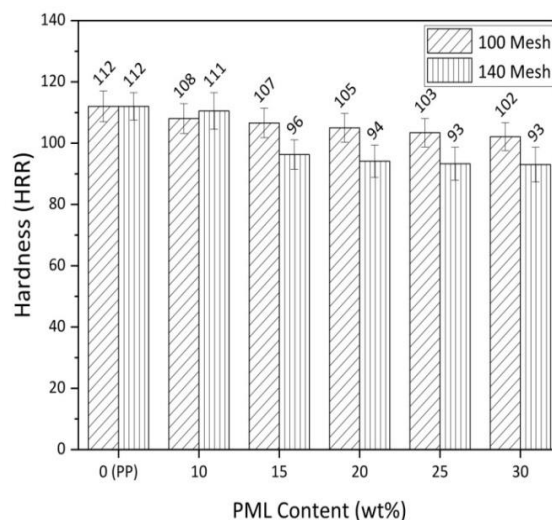


Figure 7. Hardness of PP/PML composites

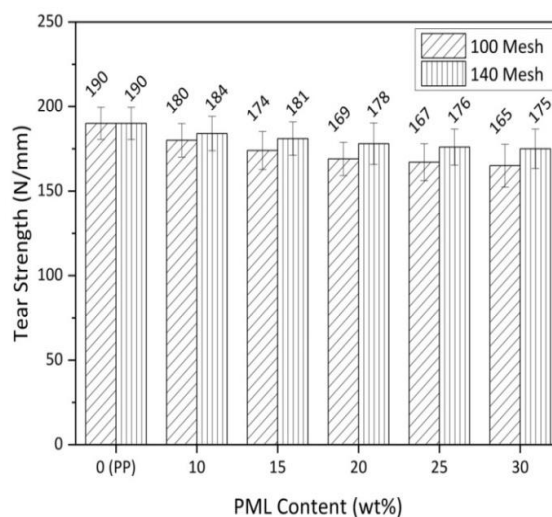


Figure 8. Tear strength of PP/PML composites

Figure 9 exhibits puncture resistance of pure PP and PP/PML composites at different PML loading. The average puncture resistance of both 100 mesh and 140 mesh PP/PML composites was lower compared to the puncture resistance of neat PP and showed a decreasing trend with increasing PML contents. The puncture resistance obtained in this work is 400–430 N/mm for 100 mesh PML and 390–429 N/mm for 140 mesh PML, which was not significantly decreased from the puncture resistance of pure PP. It can be explained by taking into account that the tensile strength of PP/PML composites also decreased. In contrast, the puncture resistance

is highly dependent on the tensile strength and stiffness of the material (He et al., 2016). However, the puncture resistance of 100 mesh PML was more significant than the puncture resistance of 140 mesh PML; this can be attributed to 100 mesh PML providing more stiffness to the composites.

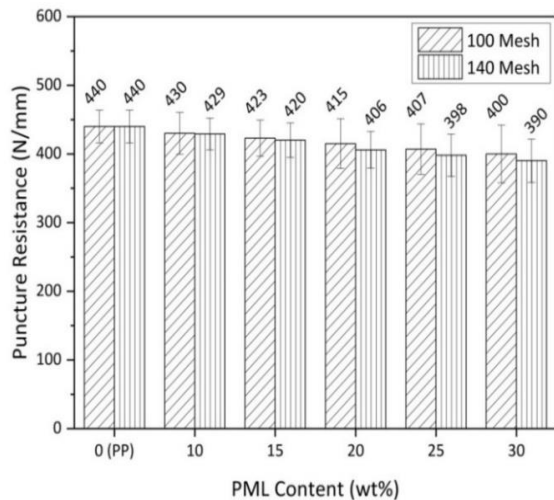


Figure 9. Puncture resistance of PP/PML composites

Thermogravimetric Analysis (TGA)

TGA thermograms of the pure PP and PP/PML composites are shown in Figures 10 a, b. The figures show a mass loss of typical composites. The weight loss observed at 50–100 °C is attributed to the evaporation of adsorbed water (~3%) from PML (Figure 10). The second weight loss in samples was due to the decomposition of the cellulose in the PML, with the maximum peak at around 229 °C (De Rosa et al., 2010). On the other hand, the PP/PML composites show a lower thermal decomposition temperature than PP. These events might be attributed to the degradation of the PML component, followed by the formation of a char residue (Mohammadkazemi et al., 2015). As seen in Figure 10, the temperature in which the maximum rate of mass loss (T_m) of PP is 445.8 °C, and T_m for composites are shifted to the higher temperatures. The higher the PML content in the composites, the higher the T_m shift. These phenomena are due to the formed-char in the heating process inhibiting the composites' PP decomposition. Similarly, Figure 10 indicates that filler particle size has no significant effects on the thermal

degradation behavior of the composites; thus thermal degradation behavior is affected by the filler contents but not by the particle size of the filler.

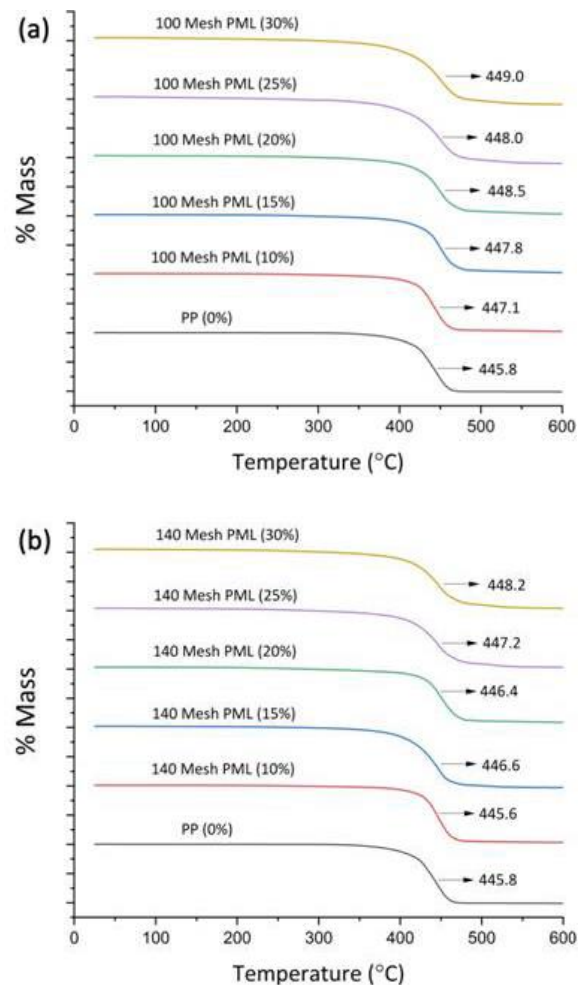


Figure 10. TGA of PP/PML composites (a) 100 mesh and (b) 140 mesh

Water Absorption Properties

The main objective of water absorption characterization was to study the effect of water absorption on the mechanical properties of the composites. Table 1 shows the effect of PML particle size and contents on the water absorption after 1, 7, 14, and 28 days of immersion. It was found that the percentage of water absorption increased with increasing filler content and immersion duration. The PML contents dominated the water absorption in these composites since the matrix PP is hydrophobic. PML contains hemicellulose, cellulose (hydrophilic), and hydrophobic lignin. The chemical composition and geometry of PML filler may affect water

absorption. The –OH (hydroxyl groups) in cellulose is the most responsible for water uptake (Lindman et al., 2017; Dórame-Miranda et al., 2019) in the composites.

The maximum water absorption for 28 days is about 7.5% smaller than wood/polypropylene composite (Gozdecki et al., 2015) with the same filler content. PML particle size and geometry of composite may also affect water absorption. A larger particle may result in more voids in the composites, and the voids, in turn, will reduce any mechanical property. The void can be minimized by controlling process parameters such as pressure, temperature, or injection techniques (Burgstaller, 2014) during the preparation test specimen. Table 1 demonstrates that the water absorption in 100 mesh PP/PML composites was higher than that of 140 mesh. It may relate to better encapsulation with polypropylene matrix for smaller filler particulate size during process preparation composites to minimize contact between water-PML. The water absorption test

specimens were prepared from the cut of the sheet, in which the surface and edge morphology are pretty different (Figures 1 and 2). Significantly few PML is observed on the specimen surface, showing a PP laminated surface. This lamination inhibited direct contact with water-PML during the immersion test. Thus, water absorption most probably occurs from the edge. The PML was a discontinuous distributed phase in the composites; it hinders access of the water molecules into the composite.

Contrary to the PML distribution, the larger particle size and porous particulate structure of PML result in easier water uptake. These PP/PML results showed more negligible water absorption than PP/ pineapple leaf (WGL) composites (Kengkhetkit & Amornsakchai, 2014) for the same filler content and immersion duration. The significant difference in water absorption of both composites is thought from different vegetation leaf, particulate size, and composite system.

Table 1. Water absorption of PP/PML composites.

PML Content	Water Absorption (%)			
	1 Day	7 Days	14 Days	28 Days
100 mesh (wt%)				
0 (Pure PP)	0	0.01	0.02	0.03 ± 0.005
10	0.68 ± 0.17	0.87 ± 0.12	1.15 ± 0.11	1.25 ± 0.12
15	0.88 ± 0.22	1.02 ± 0.21	1.52 ± 0.22	1.80 ± 0.20
20	1.03 ± 0.36	1.52 ± 0.41	2.21 ± 0.55	2.87 ± 0.56
25	1.82 ± 0.39	2.92 ± 0.52	4.18 ± 0.62	5.18 ± 0.82
30	2.41 ± 0.42	4.35 ± 0.62	6.36 ± 0.83	7.50 ± 1.22
140 mesh (wt%)				
0 (Pure PP)	0	0.01	0.02	0.03 ± 0.005
10	0.67 ± 0.16	0.85 ± 0.14	1.13 ± 0.11	1.23 ± 0.10
15	0.88 ± 0.24	1.09 ± 0.21	1.57 ± 0.22	1.81 ± 0.22
20	1.02 ± 0.46	1.52 ± 0.41	2.21 ± 0.53	2.89 ± 0.56
25	1.80 ± 0.49	2.90 ± 0.50	4.15 ± 0.58	5.16 ± 0.72
30	2.39 ± 0.41	4.31 ± 0.62	6.34 ± 0.73	7.41 ± 1.02

Table 2. Tensile strength of PP/PML composites after immersion.

PML Content	Tensile Strength (MPa)			
	1 Day	7 Days	14 Days	28 Days
100 mesh (wt%)				
0 (Pure PP)	33.0 ± 1.2	33.0 ± 1.2	33.0 ± 1.2	33.0 ± 1.2
10	28.7 ± 1.3	28.7 ± 1.3	28.5 ± 1.4	28.5 ± 1.3
15	26.0 ± 1.3	25.9 ± 1.2	25.7 ± 1.2	25.4 ± 1.2
20	24.2 ± 1.2	24.1 ± 1.2	23.9 ± 1.2	23.6 ± 1.2
25	21.5 ± 1.3	21.4 ± 1.4	21.2 ± 1.4	21.2 ± 1.4
30	19.3 ± 1.3	19.1 ± 1.3	18.7 ± 1.3	18.1 ± 1.3
140 mesh (wt%)				
0 (Pure PP)	33.0 ± 1.2	33.0 ± 1.2	33.0 ± 1.2	33.0 ± 1.2
10	29.4 ± 1.2	29.4 ± 1.2	29.2 ± 1.2	29.0 ± 1.2
15	28.6 ± 1.2	28.5 ± 1.2	28.3 ± 1.2	28.0 ± 1.2
20	26.9 ± 1.3	26.8 ± 1.3	26.6 ± 1.2	26.1 ± 1.3
25	25.8 ± 1.3	25.6 ± 1.3	25.3 ± 1.3	24.8 ± 1.3
30	24.3 ± 1.4	24.1 ± 1.4	23.8 ± 1.4	23.4 ± 1.4

Table 3. Tensile modulus of PP/PML composites after immersion.

PML Content	Tensile Modulus (MPa)			
	1 Day	7 Days	14 Days	28 Days
100 mesh (wt%)				
0 (Pure PP)	697 ± 49	697 ± 50	696 ± 47	695 ± 49
10	971 ± 90	969 ± 90	960 ± 88	950 ± 87
15	935 ± 91	929 ± 90	920 ± 92	912 ± 94
20	950 ± 94	945 ± 92	940 ± 93	930 ± 90
25	968 ± 102	960 ± 101	950 ± 99	940 ± 97
30	970 ± 97	959 ± 99	949 ± 97	937 ± 101
140 mesh (wt%)				
0 (Pure PP)	697 ± 49	697 ± 50	696 ± 47	695 ± 49
10	938 ± 73	932 ± 75	928 ± 77	922 ± 74
15	1.028 ± 88	1.000 ± 85	1.000 ± 84	950 ± 83
20	1.022 ± 92	1.015 ± 94	1.000 ± 95	960 ± 97
25	1.060 ± 98	1.040 ± 92	1.030 ± 95	980 ± 89
30	1.040 ± 87	1.030 ± 91	1.010 ± 86	970 ± 90

Effect of Water Absorption on Tensile Properties

Tables 2 and 3 present the composites' tensile properties after 1, 7, 14, and 28 days of

water immersion. Samples for these tests were dumbbell-punch-cut of the specimens after water absorption. The edge of the dumbbell-shaped was ca. 6 mm from the edge of the

water absorption specimens. In all samples, the tensile strength and modulus slightly decrease after the immersion. After the first and seventh days of immersion, the tensile strength and modulus were not significantly decreased. It is due to negligible water absorption in the composite sheet where the dumbbell was taken. The absorbed water may not reach the dumbbell area yet for this duration of the immersion test since far from the edge. The morphology of upper and bottom surface samples is smooth like PP laminated. The water immersion did not significantly affect the tensile strength and modulus for these days. These facts were following low water absorption data in Table 1. The weaker water absorption effect than expected influences of PML contents on the tensile strengths and modulus may be attributed to the geometry and morphology of the composite surfaces. The relatively low water uptake presented in Table 1 may not result in any damage (such as swelling or micro-cracking) in the PP continuous matrix of the composites. Such material design composites should be considered for applying single-use articles on viewpoint sustainable and environmentally advantageous.

4. CONCLUSIONS

It was demonstrated that mango leaf could be utilized for filler in polypropylene/powdered mango leaf composites, using a simple preparation and processing step. It is observed that the composites' mechanical properties are relatively decreased compared with that of PP, except for the tensile and flexural modulus increase. Composites with 140 mesh PML have better physical and mechanical properties than 100 mesh. It can be concluded that the cellulose dominates PP/PML composite's water absorption behavior as the hydrophilic component contained in the PML. The discontinuous hydrophilic filler system in the composites is an advantage in preventing water absorption. A possibility of adjusting the composites' properties by varying the PML particle size and fraction can be implemented in the plastic industry. Regarding a slight decrease of some mechanical properties, advantage water absorption, and duration service of mostly single-used articles mentioned above, the composites can be easily implemented in utilizing single-used articles.

ACKNOWLEDGMENTS

This work was supported by the Indonesian Institute of Sciences (LIPI). Reference number: 12/A/IPT.7/2017.

DECLARATIONS

Competing Interest

The authors declare that they have no conflict of interest.

REFERENCES

- Abdullah, M. Z., & Aslan, N. H. C. (2019). Performance evaluation of composite from recycled polypropylene reinforced with mengkuang leaf fiber. *Resources*, 8(2). <https://doi.org/10.3390/resources8020097>
- Ahmed, A. S., Islam, M. S., Hassan, A., Mohamad Haafiz, M. K., Islam, K. N., & Arjmandi, R. (2014). Impact of succinic anhydride on the properties of jute fiber/polypropylene biocomposites. *Fibers and Polymers*, 15(2), 307–314. <https://doi.org/10.1007/s12221-014-0307-8>
- Amin, M. R., Chowdhury, M. A., & Kowser, M. A. (2019). Characterization and performance analysis of composite bioplastics synthesized using titanium dioxide nanoparticles with corn starch. *Heliyon*, 5(8). <https://doi.org/10.1016/j.heliyon.2019.e02009>
- Bilal, A., Lin, R. J. T., & Jayaraman, K. (2014). Effects of fibre loading and interfacial modification on physical properties of rice husk /PE composites. *Applied Mechanics and Materials*, 575, 223–226. <https://doi.org/10.4028/www.scientific.net/AMM.575.223>
- Burgstaller, C. (2014). A comparison of processing and performance for lignocellulosic reinforced polypropylene for injection moulding applications. *Composites Part B: Engineering*, 67, 192–198. <https://doi.org/10.1016/j.compositesb.2014.07.010>
- Das, S. P., Ghosh, A., Gupta, A., Goyal, A., & Das, D. (2013). Lignocellulosic fermentation of wild grass employing recombinant hydrolytic enzymes and fermentative microbes with effective bioethanol recovery. *BioMed Research International*, 2013. <https://doi.org/10.1155/2013/386063>
- De Rosa, I. M., Kenny, J. M., Puglia, D., Santulli, C., & Sarasini, F. (2010). Morphological,

- thermal and mechanical characterization of okra (*Abelmoschus esculentus*) fibres as potential reinforcement in polymer composites. *Composites Science and Technology*, 70(1), 116–122. <https://doi.org/10.1016/j.compscitech.2009.09.013>
- Delville, J., Joly, C., Dole, P., & Bliard, C. (2003). Influence of photocrosslinking on the retrogradation of wheat starch based films. *Carbohydrate Polymers*, 53(4), 373–381. [https://doi.org/10.1016/S0144-8617\(03\)00141-3](https://doi.org/10.1016/S0144-8617(03)00141-3)
- Dórame-Miranda, R. F., Gámez-Meza, N., Medina-Juárez, L. Á., Ezquerra-Brauer, J. M., Ovando-Martínez, M., & Lizardi-Mendoza, J. (2019). Bacterial cellulose production by *Gluconacetobacter entanii* using pecan nutshell as carbon source and its chemical functionalization. *Carbohydrate Polymers*, 207, 91–99. <https://doi.org/10.1016/j.carbpol.2018.11.067>
- Dordević, N., Marinković, A. D., Nikolić, J. B., Drmanić, S., Rančić, M., Brković, D. S., & Uskoković, P. S. (2016). A study of the barrier properties of polyethylene coated with a nanocellulose/magnetite composite film. *Journal of the Serbian Chemical Society*, 81(5), 589–605. <https://doi.org/10.2298/JSC151217019D>
- Gozdecki, C., Wilczyński, A., Kociszewski, M., & Zajchowski, S. (2015). Properties of wood–plastic composites made of milled particleboard and polypropylene. *European Journal of Wood and Wood Products*, 73(1), 87–95. <https://doi.org/10.1007/s00107-014-0852-2>
- He, G., Zhang, F., Yu, H., Li, J., & Guo, S. (2016). Puncture characterization of multilayered polypropylene homopolymer/ethylene 1-octene copolymer sheets. *RSC Advances*, 6(16), 12744–12752. <https://doi.org/10.1039/c5ra23333j>
- Indra Reddy, M., Anil Kumar, M., & Rama Bhadri Raju, C. (2018). Tensile and Flexural properties of Jute, Pineapple leaf and Glass Fiber Reinforced Polymer Matrix Hybrid Composites. *Materials Today: Proceedings*, 5(1), 458–462. <https://doi.org/10.1016/j.matpr.2017.11.105>
- Kengkhetkit, N., & Amornsakchai, T. (2014). A new approach to “Greening” plastic composites using pineapple leaf waste for performance and cost effectiveness. *Materials and Design*, 55, 292–299. <https://doi.org/10.1016/j.matdes.2013.10.005>
- Kocak, D., & Mistik, S. I. (2015). The use of palm leaf fibres as reinforcements in composites. *Biofiber Reinforcements in Composite Materials*, 273–281. <https://doi.org/10.1533/9781782421276.2.273>
- Lindman, B., Medronho, B., Alves, L., Costa, C., Edlund, H., & Norgren, M. (2017). The relevance of structural features of cellulose and its interactions to dissolution, regeneration, gelation and plasticization phenomena. *Physical Chemistry Chemical Physics*, 19(35), 23704–23718. <https://doi.org/10.1039/c7cp02409f>
- Marichelvam, M. K., Jawaid, M., & Asim, M. (2019). Corn and rice starch-based bioplastics as alternative packaging materials. *Fibers*, 7(4), 1–14. <https://doi.org/10.3390/fib7040032>
- Mazerolles, T., Heuzey, M. C., Soliman, M., Martens, H., Kleppinger, R., & Huneault, M. A. (2019). Development of co-continuous morphology in blends of thermoplastic starch and low-density polyethylene. *Carbohydrate Polymers*, 206(November 2018), 757–766. <https://doi.org/10.1016/j.carbpol.2018.11.038>
- Medina-Jaramillo, C., Ochoa-Yepes, O., Bernal, C., & Famá, L. (2017). Active and smart biodegradable packaging based on starch and natural extracts. *Carbohydrate Polymers*, 176(August), 187–194. <https://doi.org/10.1016/j.carbpol.2017.08.079>
- Mir, S. S., Nafsin, N., Hasan, M., Hasan, N., & Hassan, A. (2013). Improvement of physico-mechanical properties of coir-polypropylene biocomposites by fiber chemical treatment. *Materials and Design*, 52, 251–257. <https://doi.org/10.1016/j.matdes.2013.05.062>
- Mohammadkazemi, F., Azin, M., & Ashori, A. (2015). Production of bacterial cellulose using different carbon sources and culture media. *Carbohydrate Polymers*, 117, 518–523. <https://doi.org/10.1016/j.carbpol.2014.10.008>
- Nguyen, D. M., Do, T. V. V., Grillet, A. C., Ha Thuc, H., & Ha Thuc, C. N. (2016). Biodegradability of polymer film based on low density polyethylene and cassava starch. *International Biodeterioration and Biodegradation*, 115, 257–265.

<https://doi.org/10.1016/j.ibiod.2016.09.004>

- Rahman, M. R., Huque, M. M., Islam, M. N., & Hasan, M. (2008). Improvement of physico-mechanical properties of jute fiber reinforced polypropylene composites by post-treatment. *Composites Part A: Applied Science and Manufacturing*, 39(11), 1739–1747. <https://doi.org/10.1016/j.compositesa.2008.08.002>
- Roy, S. B., Ramaraj, B., Shit, S. C., & Nayak, S. K. (2011). Polypropylene and potato starch biocomposites: Physicomechanical and thermal properties. *Journal of Applied Polymer Science*, 120(5), 3078–3086. <https://doi.org/10.1002/app.33486>
- Sadeghifar, H., & Argyropoulos, D. S. (2016). Macroscopic Behavior of Kraft Lignin Fractions: Melt Stability Considerations for Lignin-Polyethylene Blends. *ACS Sustainable Chemistry and Engineering*, 4(10), 5160–5166. <https://doi.org/10.1021/acssuschemeng.6b00636>
- Satoto, R., Karina, M., Hanif, A., Abdullah, D., & Nugroho, P. (2019). Mechanical and degradability properties of polyethylene / PBL composites in a wet-dry controlled environment. *Journal of Materials and Environmental Science*, 10(8), 706–718.
- Scaffaro, R., Lopresti, F., & Botta, L. (2018). PLA based biocomposites reinforced with *Posidonia oceanica* leaves. *Composites Part B: Engineering*, 139(November 2017), 1–11. <https://doi.org/10.1016/j.compositesb.2017.11.048>
- Wang, S., Feng, N., Zheng, J., Yoon, K. B., Lee, D., Qu, M., Zhang, X., & Zhang, H. (2016). Preparation of polyethylene/lignin nanocomposites from hollow spherical lignin-supported vanadium-based Ziegler–Natta catalyst. *Polymers for Advanced Technologies*, 27(10), 1351–1354. <https://doi.org/10.1002/pat.3803>
- Zhang, Q., Yi, W., Li, Z., Wang, L., & Cai, H. (2018). Mechanical properties of rice husk biochar reinforced high density polyethylene composites. *Polymers*, 10(3), 1–10. <https://doi.org/10.3390/polym10030286>